Carbohydrate Research 401 (2015) 16–23

Contents lists available at ScienceDirect

Carbohydrate Research

journal homepage: www.elsevier.com/locate/carres

Supercritical water treatment for cello-oligosaccharide production from microcrystalline cellulose

Lasse K. Tolonen [a], Minna Juvonen [b], Klaus Niemelä [c], Atte Mikkelson [c], Maija Tenkanen [b], Herbert Sixta [a,*]

[a] Aalto University, Department of Forest Products Technology, PO Box 16300, FI-00076 Aalto, Finland
[b] Department of Food and Environmental Sciences, PO Box 27, FI-00014 University of Helsinki, Finland
[c] VTT, PO Box 1000, FI-02044 VTT, Finland

ARTICLE INFO

Article history:
Received 28 August 2014
Received in revised form 15 October 2014
Accepted 17 October 2014
Available online 25 October 2014

Keywords:
Biorefinery
Supercritical water
Cellulose
Oligosaccharide
Prebiotics

ABSTRACT

Microcrystalline cellulose was treated in supercritical water at 380 °C and at a pressure of 250 bar for 0.2, 0.4, and 0.6 s. The yield of the ambient-water-insoluble precipitate and its average molar mass decreased with an extended treatment time. The highest yield of 42 wt % for DP2-9 cello-oligosaccharides was achieved after the 0.4 s treatment. The reaction products included also 11 wt % ambient-water-insoluble precipitate with a DP_w of 16, and 6.1 wt % monomeric sugars, and 37 wt % unidentified degradation products. Oligo- and monosaccharide-derived dehydration and retro-aldol fragmentation products were analyzed via a combination of HPAEC-PAD–MS, ESI-MS/MS, and GC–MS techniques. The total amount of degradation products increased with treatment time, and fragmented (glucosyl$_n$-erythrose, glucosyl$_n$-glycolaldehyde), and dehydrated (glucosyl$_n$-levoglucosan) were identified as the main oligomeric degradation products from the cello-oligosaccharides.

1. Introduction

Cellulose, being globally and abundantly available, is probably the most important biopolymer that is currently used in a wide variety of applications such as paper products, textile fibers and for the production of biofuels and platform chemicals.[1] Cellulose is also the natural source for the manufacture of cello-oligosaccharides. In general, oligosaccharides are water-soluble saccharide polymers, typically consisting of two to ten monosaccharide units, although the definition varies. An example of the possible applications for oligosaccharides is their use as prebiotics that are added in increasing quantities to foods with the focus on beverages and milk products.[2–4] By definition, prebiotics are food ingredients that are not digested by humans and have zero metabolizable energy value. Instead they provide a source of carbon for the intestinal microflora stimulating the beneficial bacteria in the colon.[2] Not all oligosaccharides are, however, recognized or used as prebiotics and this applies also to cello-oligosaccharides.[2] Yet there is a reason to believe that cello-oligosaccharides are potential prebiotics because the human digestion system lacks the enzyme that is required to hydrolyze the β-glucosidic bond in the cello-oligosaccharides.[3] Fermentation activity in the human intestine was reported for cellobiose indicating that it acts as energy source for certain bacteria.[5]

An obvious reason for the lack of extensive research on cello-oligosaccharides is their limited availability and high price, which is caused by cellulose's recalcitrant nature compared with other polysaccharides like starch. Cellulose is a linear polysaccharide consisting of β(1 → 4) linked D-anhydroglucopyranose units (AGU) in which every second AGU is rotated 180° in the plane, adjacent units forming a cellobiose. Cellulose exists as a polymer with the degree of polymerization (DP) up to 10,000 AGUs.[1] In the naturally existing cellulose I allomorph, the cellulose chains are aligned parallel, forming sheets which are stacked on top of each other, thus forming ordered crystalline domains interrupted by less ordered domains.[1] In the crystalline domains, a rigid intra and interchain hydrogen bond network is formed in the cellulose sheets whereas these sheets are held together by Van der Waals—forces which were in fact reported to be the pivotal factor for cellulose recalcitrance.[6] Also hydrophobic interaction, which is caused by the affinity of water molecules to each other, is important regarding the insolubility of cellulose in aqueous systems.[7] As a result, in order to produce water-soluble cello-oligosaccharides, the cellulose must be depolymerized in a controlled manner which will render it water-soluble. The challenge is to hydrolyze cellulose as oligomers instead of obtaining mere monomers, which

* Corresponding author. Tel.: +358 503841746.
E-mail addresses: lasse.tolonen@aalto.fi (L.K. Tolonen), minna.juvonen@helsinki.fi (M. Juvonen), klaus.niemela@vtt.fi (K. Niemelä), atte.mikkelson@vtt.fi (A. Mikkelson), maija.tenkanen@helsinki.fi (M. Tenkanen), herbert.sixta@aalto.fi (H. Sixta).

http://dx.doi.org/10.1016/j.carres.2014.10.012
0008-6215/

is typically not possible via acid-catalyzed hydrolysis at near-ambient temperatures. Therefore, a separate dissolution step is typically needed to create a homogeneous environment for the hydrolysis of cellulose to oligosaccharides.

In the early 1990s it was discovered that crystalline cellulose can be converted to water-soluble species via a noncatalytic subcritical or supercritical water treatment.[8] This process has the advantage that the hydrolyzed cellulose is dissolved not as a monomer but rather as oligomers or short polymers whose DP depends on the treatment temperature.[9] No actual swelling and dissolution of the cellulose crystallites take place in subcritical water at least below 300 °C,[10] while at temperatures higher than 300 °C and at a pressure of 25 MPa, a crystalline-to-amorphous transformation was reported.[11] This transformation results in a rapid destruction of the crystallites in near critical and supercritical water.[12–14] When the temperature reaches the critical point (374 °C and 22.1 MPa) at a pressure of 25 MPa, the internal energy of the system increases almost stepwise and the physical properties of water are drastically changed. These factors were attributed to a stepwise acceleration of cellulose dissolution.[12,14] Overall, the rate of cellulose dissolution increases faster than the corresponding rate of degradation of sugar, which enables the recovery of the dissolved compounds in high yields.[12]

Although supercritical water treatment was shown to dissolve and hydrolyze cellulose in one stage without a dedicated cellulose solvent, several degradation reactions concomitantly occur during the supercritical water treatment. These formed reaction products may have an effect on the use of the produced oligosaccharides in applications where a high purity is required. In subcritical water the proton concentration is higher than in ambient water catalyzing hydrolytic depolymerization and dehydration; in near- and supercritical water dehydration and fractionation via retro-aldol reactions become more prominent favoring reaction products such as levoglucosan, 5-hydroxymethylfurfural, erythrose, methylglyoxal, glycolaldehyde, and dihydroxyacetone.[12,15,16] These degradation reactions are not restricted to monosaccharides but take place also at the reducing end groups of polysaccharides.[17]

In this study we investigated the dissolution and depolymerization of microcrystalline cellulose to water-soluble cello-oligosaccharides and the formation of degradation products thereof. The yields and molar mass distributions were determined from ambient-water-soluble oligosaccharides and cellulose precipitate which was insoluble in ambient water. The formed monomeric and oligomeric degradation products were investigated by HPAEC-PAD–MS, ESI-MS/MS, and GC–MS techniques.

2. Experimental

Commercial microcrystalline cellulose (MCC) powder was purchased from Merck and used as raw material. The mass average molar mass of the MCC was 32.9 kg mol^{-1} and polydispersity index 2.03.[10] The carbohydrate composition of the MCC after total hydrolysis was 97.8% glucose, 1.0% xylose, and 1.2% mannose, analyzed by HPAEC-PAD with a CarboPac PA20 column after the hydrolysis to monosugars as described earlier.[18] Water–MCC suspension was prepared by mixing the MCC powder thoroughly with deionized water. Nitrogen purging was applied in order to remove oxygen from the suspension. The prepared cellulose suspension was treated with a bench-scale tubular flow reactor system described earlier.[13] Three experiments were conducted at the temperature of 380 °C employing treatment times of 0.20 s, 0.40 s, and 0.60 s. The pressure was held at 25.0 MPa in all experiments. The concentration of the cellulose suspension was 0.50 wt % in the feeding tank and 0.20 wt % in the beginning of the supercritical water treatment after dilution by supercritical heating water.

The overall sampling and analysis procedure is illustrated in Scheme 1. In order to avoid the earlier reported problem with the re-deposition of precipitated cellulose, the time required for the removal of the undissolved residue was reduced to approximately 15 s.[13] The solution from the reactor's outlet was taken into a 10 mL syringe and immediately pressed through a syringe filter (Acrodisk, PN4523T). In total 50 mL of reaction product solution was filtered in this way. The syringe filters were then dried at 105 °C, and the amount of undissolved cellulose residue was determined gravimetrically. The filtered solution was stored in a cold room to allow the precipitation of cellulose take place. The formed precipitate was separated by centrifugation for analytical size exclusion chromatography.

Besides the samples collected with the syringe filters, several liters of reaction solution were collected and stored in a cold room for more than 48 h. During that time nearly all of the dissolved cellulose chains precipitated. The solid fraction containing the undissolved residue and the formed precipitate was removed using filters (Whatman Polycap heavy duty 5.0/10.0 μm). The filters were dried overnight at 105 °C and the total amount of undissolved residue and precipitate was determined gravimetrically. The amount of cellulose precipitate was obtained by subtracting the amount of undissolved residue from the total amount of residue and precipitate.

A part of the 0.4 s treated, filtrated sample was fractionated by preparative-scale size exclusion chromatography (Prep-SEC). First the sample was concentrated to 1:20 of its volume by a rotary evaporator (55 °C and 80 mbar) to compensate for the dilution in

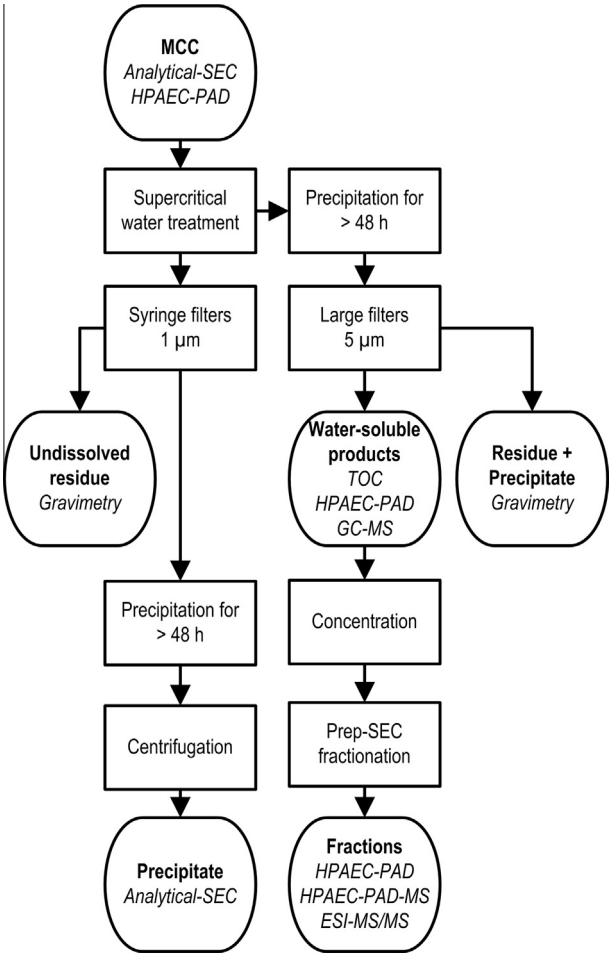

Scheme 1. Experimental procedure. Conducted analyses indicated by italics.

the subsequent Prep-SEC in which it was fractioned to 93 fractions, 10.3 mL each, using Bio-Gel P-2 (Bio-Rad) column (height and diameter 94 cm and 5 cm, respectively) with a particle size of 45–90 μm. The Prep-SEC fractionation was done at room temperature, and degassed MilliQ-water was used as eluent. A flow rate of 0.9 mL min^{-1} was applied.

The molar mass of the polymers in the precipitate was determined by analytical size exclusion chromatography (SEC). A solvent exchange sequence [water–acetone–*N*,*N*-dimethylacedamide (DMAc)] was carried out in 2 mL Eppendorf-tubes using centrifugation for the separation of the precipitate and solvent. The samples were dissolved in 90 g L^{-1} anhydrous lithium chloride (LiCl)/DMAc at room temperature under occasional shaking, diluted according to their estimated concentration to 1.0 g L^{-1}, and filtered with 0.2 μm syringe filters. The SEC-analysis was performed with a Dionex Ultimate 3000 chromatography system that comprised one guard column (PLgel Mixed-A, 7.5 × 50 mm, Agilent Technologies) and four analytical columns (PL-gel Mixed-A, 7.5 × 300 mm) in series and an RI-detector (Shodex RI-101). The analysis was carried out at room temperature using 9 g L^{-1} LiCl/DMAc solution as the eluent (0.75 mL min^{-1}). Double injections were conducted for each sample (100 μL). Narrow pullulan standards (343 Da–708 kDa, Polymer Standard Service GmbH, and 1600 kDa, Fluka GmbH) were used to calibrate the system. The molar mass distributions were calculated by using a MATLAB script written at Aalto University.

High-performance anion exchange chromatography system (Dionex ICS-3000) with pulsed amperometric detection (HPAEC-PAD) was employed for the analysis of water-soluble oligo- and monomers. The system comprised one Carbopac PA100 guard column and an analytical column of similar type. Flow rate of 0.600 mL min^{-1} and temperature of 22 °C were applied. The eluent concentration was 100 mM for NaOH(aq) throughout all the runs. The linear NaOAc gradients for the analysis of the oligosugar fractions was 10, 10, 200, 250, 50, and 50 mM at 0, 3, 30, 31, 35, 36, and 45 min, respectively. The SEC-fractions were analyzed using a modified linear eluent profile in which the NaOAc profile was 15, 15, 200, 250, 50, and 50 mM at 0, 10, 30, 31, 35, 36, and 45 min, respectively. Cellotriose (~95%), cellotetraose (~95%), cellopentaose (~95%), and cellohexaose ~90% from Megazyme and D(+)-glucose, p.a. and D(+)-cellobiose (Fluka 22150-10G, >99%) were used to calibrate the analysis. Flory–Schulz type distributions ($c(x) = bx(1-a)^{x-1}$) where c is concentration as a function of x which is degree of polymerization, and a and b are constants) were fitted to the observed oligosaccharide concentrations using the MATLAB's curve fit toolbox.

The negative ion mass spectrometry experiments of isolated DP3 and DP4 fractions were performed with Agilent XCT Plus model quadrupole ion trap mass spectrometer, equipped with an electrospray ionization source (Agilent Technologies) (ESI-MS/MS). Five microliter aliquots of the fractions were diluted with 50% methanol (v/v) to a final volume of 200 μL. Standard samples, cellotriose and cellotetraose, were diluted with 50% methanol (25 μg mL^{-1}). Ammonium chloride was added (50 μg mL^{-1}) for $[M+Cl]^-$-adduct ion formation. Sample and standard solutions were infused into the ESI source at a flow rate of 5 μL min^{-1} via a syringe pump. The electron spray capillary voltage was set to 3200 V and end plate off set to −500 V. Other parameters were set automatically by target ion mass (m/z 539 for DP3 fraction and m/z 701 for DP4 fraction). Nitrogen gas was used as both nebulizing gas and drying gas. The drying gas temperature was set to 325 °C. The drying gas was flow 4 L min^{-1} and nebulizer pressure was 1.03 bar (15 psi). The range of m/z 100–1500 was scanned and 5 scans were averaged for a spectrum. Each spectrum was produced by accumulating data for 1 min. In MS/MS analysis the fragmentation amplitude for collision-induced dissociation (CID) was 0.45–0.55 V. Mass spectra were processed using DataAnalysis software (Bruker Daltonik GmbH).

The DP3 and DP4 fractions were also analyzed by Dionex ICS ICS-3000 system coupled to a MSQ Plus mass spectrometer (Thermo Scientific Dionex) (HPAEC-PAD–MS). The samples were analyzed without pretreatment after fractionation by preparative-SEC. The analytes were separated using a CarboPac PA200 column (3 mm × 250 mm) together with a CarboPac PA200 guard column (3 mm × 50 mm, DionexCorp, USA) at 30 °C using flow rate 0.3 mL min^{-1}. After injection of a 100 μL sample (filtered with a 0.45 μm filter), 100 mM NaOH was run through the column for 5 min, after which gradient of 100 mM to 300 mM NaOAc/100 mM NaOH in 33 min was applied. Then column was washed with 100 mM NaOH/300 mM NaOAc and 300 mM NaOH. After the analytical column, a T-piece diverted one part of the flow directly to pulsed amperometric detection (PAD) while the other part of the eluent was desalted through a Thermo Scientific Dionex ASRS suppressor. After the suppressor, the eluent was mixed with a solution of lithium chloride (500 μmol L^{-1}) via second T-piece in order to detect carbohydrates by mass spectrometry as lithium adducts. The positive electrospray ionization-single quadrupole mass spectrometer was operated at the following conditions: probe temperature 400 °C, nitrogen pressure, cone voltage 90 V, needle voltage 3 kV and scan range of 100–1050 m/z was applied. The delay times of both detectors were synchronized automatically by the Chromeleon software package.

Unfractionated water-soluble products were analyzed by GC–MS as their trimethylsilyl (TMS) derivatives, for the determination of the monomeric degradation products additional to glucose. The applied procedure and equipment are described in[19] together with references to relevant mass spectral data. Additional references were now consulted for the final identification of glycolaldehyde in cyclic forms and erythrose.[20,21]

3. Results and discussion

3.1. Undissolved residue and cellulose precipitate

Supercritical water treatment at 380 °C resulted in the rapid decomposition of the microcrystalline cellulose. In the supercritical water treatment and the subsequent separation steps, microcrystalline cellulose was fractioned into *undissolved residue*, cellulose chains that dissolved in supercritical water but precipitated in ambient water, denoted hereafter as *precipitate*, and *water-soluble compounds*. The shares of these fractions depended on the treatment conditions (Table 1). After the 0.2 s treatment, a small amount of solid matter was recovered. This fraction was considered to be undissolved crystalline cellulose residue although its low quantity did not allow for analyzing whether the residue had retained cellulose Iβ allomorph. After the 0.4 s and 0.6 s treatments no solid residue was found, indicating a complete dissolution of the cellulose crystallites.

The formation of white precipitate was observed a few minutes after the solution was recovered from the reactor system and continued for hours. This precipitating fraction has been earlier identified as cellulose II allomorph, showing that it originates from completely dissolved cellulose chains.[12,13,17,22] The yield and molar mass of the cellulose precipitate depended on the treatment time: a longer treatment time resulted in a lower yield of precipitate (Tables 1 and 2). This is explained by the depolymerization of the dissolved chain, which was observed as the shifted molar mass distributions, reducing the degree of polymerization below the solubility limit of cellulose therefore rendering the chains water-soluble (Table 2).

Table 1
The main fractions and identified water-soluble compounds from supercritical water treatment as percentages on initial microcrystalline cellulose with different treatment times

	0.2 s	0.4 s	0.6 s
Main fractions			
Undissolved residue	8	0	0
Precipitate	35	11	<1
Water-soluble comp.[a]	57	89	100
Total concentration	922	1100	1024
Identified constituents			
DP2-9 COS[b]	29	42	30
Glucose[b]	2.4	5.0	7.7
Xylose[b]	0.3	0.5	0.5
Mannose[b]	0.2	0.3	0.4
Fructose[b]	0.1	0.3	0.5
Degradation products[c]	2.1	3.5	3.5
Unident. constituents[d]	23	37	57

[a] From TOC as anhydroglucan + gravimetric analyses of undissolved residue and precipitate.
[b] HPAEC-PAD with a PA20 column.
[c] GC–MS (see Table 3).
[d] Calculated from the mass balance.

Table 2
Molar mass averages of cellulose precipitate (g mol^{-1}) with different treatment times.

	0.2 s	0.4 s	0.6 s
Number average	2072	1851	1560
Mass average	3238	2643	1917
$DP_{5\%}$[a]	6	6	5
$DP_{95\%}$[b]	47	36	21
Polydispersity index	1.6	1.4	1.2

[a] 5% of precipitate has a lower DP. Rounded up to next integer.
[b] 95% of precipitate has a lower DP. Rounded down to next integer.

The analytical-SEC revealed that after the 0.2 s treatment 90 wt % of the cellulose precipitate comprised fractions between DP9 and DP47 (Table 2), and the molar mass distribution was shifted toward a low molar mass with a prolonged treatment time. In general, the average molar masses of cellulose precipitate determined in this study were lower than those reported by Sasaki et al.[12] or Ehara and Saka[17] who reported viscosity average values at around DP50-30 and a distribution from DP13 to DP100, respectively. Caution is required in particular with the low and high molar mass tails in the distribution because those may be affected by the band-broadening effect.[23]

The number-weighted average molar mass decreased nearly linearly against the reciprocal treatment time, suggesting that depolymerization occurs randomly in supercritical water. In this case the resulting polydispersity index for high polymers would be two.[24] However, the PDI values are clearly lower than 2 (Table 2), probably due to a fractionation upon precipitation, which automatically results in a truncated molar mass distribution of precipitate.

3.2. Water soluble cello-oligosaccharides

The fraction that remained soluble in ambient water was quantified based on the carbon balance (Table 1). The cello-oligosaccharides together with monomeric glucose, which are the primary depolymerization products of cellulose, were detected and quantified by HPAEC-PAD analysis. The reliable quantification of all detected oligosaccharide peaks was challenging because commercial calibration standards were not available beyond DP6. Hence we used an approach described by Yu and Wu,[22] where the response factors (nC mg^{-1}) were obtained from the slopes of calibration lines of the existing DP2-6 standards and these known response factors were then extrapolated to the DP7-9. In order to avoid problems with integration in the presence of several side peaks, the calibration and analysis was done against the peak heights.

The concentrations of the identified water-soluble oligosaccharides were clearly affected by the treatment time: the total quantity of water-soluble oligosaccharides increased from 29% after 0.2 s to 42% after 0.4 s (Table 1 and Fig. 1) but decreased when the treatment was extended to 0.6 s. The increase in total oligosaccharide concentration between the 0.2 s and 0.4 s treatments is undoubtedly due to the depolymerization of longer chains, which was seen as the decreasing molar mass and amount of the precipitate. The concentrations of DP1-6 cello-oligosaccharides were used to fit Flory–Schulz distributions in Figure 1. Good agreement between the measured data and the distributions supports the random depolymerization mechanism. In addition, the Flory–Schulz distributions match well with the DP7-9 concentrations thereby indicating that the extended calibration was valid. The parallel analysis using a PA20 column revealed only low concentrations of xylose, mannose, and fructose (Table 1), and verified the glucose concentrations from the oligomer analysis (Fig. 1).

3.3. Dehydration and retro-aldol fragmentation products

A large number of smaller unidentified peaks were detected in the HPAEC-PAD analysis. In order to get more information on the other oligomeric products, the sample treated for 0.4 s was fractionated with Prep-SEC and the fractions were analyzed by HPAEC-PAD. The contour map in Figure 2 revealed a series of the main oligomer peaks that eluted according to their DP. The main cello-oligosaccharide peaks of each fraction exhibited a bimodal shape (insert in Fig. 2) which was reported earlier.[22] In addition to the bimodal main peak, two substantial side peaks were detected for each cello-oligosaccharide together with several unidentified peaks in the monosugar range. No oligosaccharides above DP8 were found in the analyzed fractions, and it is probable that they precipitated during the storage time and the concentration step prior to the Prep-SEC fractionation. The slight bending of peaks seen in Figure 2 was probably due to the drift of the pH because we used high injection concentrations to ensure the detection of all side peaks.

To identify the different oligomeric degradation products from cellulose, DP3 and DP4 fractions were analyzed with the ESI-MS on the negative mode as chloride adducts (Fig. 3). The base peaks

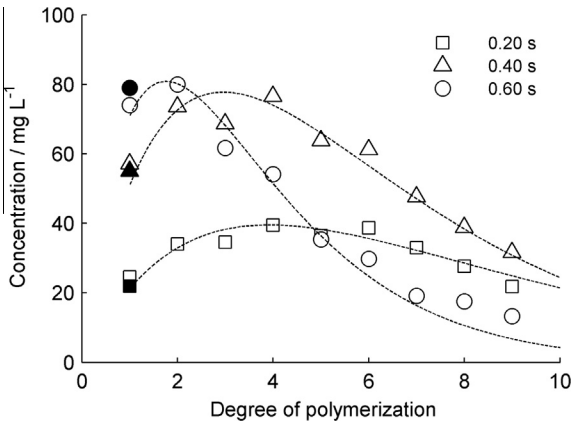

Figure 1. Analyzed cello-oligosaccharide concentrations. White markers: oligomer analysis by a PA100 column. Black markers: Monomer analysis by a PA20 column. Dashed lines represent Flory–Schulz type of molar mass distributions fitted on the DP1-6 oligosaccharide concentrations.

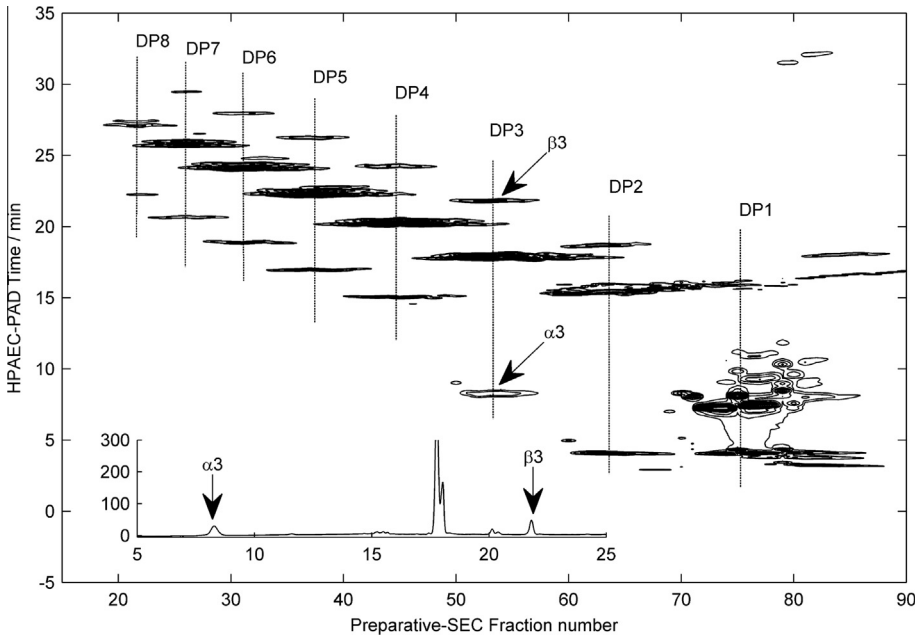

Figure 2. Contour map of Prep-SEC–HPAEC-PAD analysis for the fractions treated for 0.4 s at 380 °C. The insert shows the chromatogram of the fraction 53, *x*-axis time (min), *y*-axis signal (nC). The minimum contour level 10 nC, baseline signal subtracted from the signal. The α and β peaks are discussed in the text.

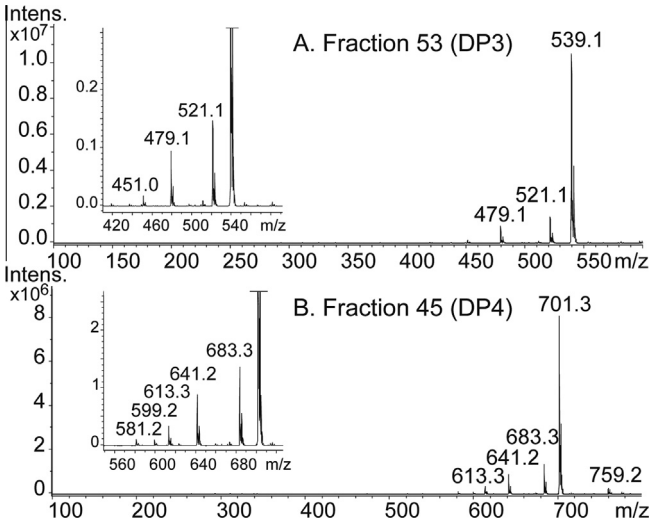

Figure 3. ESI-MS spectra of fraction 53 (A) and fraction 45 (B) as chloride anion adducts. The base peaks were identified as cellotriose (*m*/*z* 539) in the DP3 fraction and as cellotetraose (*m*/*z* 701) in the DP4 fraction. In fraction 53 (DP3) minor peaks were identified as 1,6-anhydro-β-D-cellotriose (*m*/*z* 521, $[Glc3-18\ Da+Cl]^-$), cellobiose–erythrose (*m*/*z* 479, $[Glc3-60\ Da+Cl]^-$), and cellobiose–glycolaldehyde (*m*/*z* 451, $[Glc3-120\ Da+MeOH+Cl]^-$). In fraction 45 (DP4) minor peaks were cellotetraose (*m*/*z* 759 $[Glc4+NaCl+Cl]^-$), 1,6-anhydro-β-D-cellotetraose (*m*/*z* 683, $[Glc4-18\ Da+Cl]^-$), cellotriose–erythrose (*m*/*z* 641, $[Glc4-60\ Da+Cl]^-$), and cellotriose–glycolaldehyde (*m*/*z* 613, $[Glc4-120\ Da+MeOH+Cl]^-$, *m*/*z* 599 $[Glc4-120\ Da+H_2O+Cl]^-$ and *m*/*z* 581 $[Glc4-120\ Da+Cl]^-$). Small amounts of DP_{n+1} compounds were also detected outside of currently presented spectrum range.

in the spectra were *m*/*z* 539 and *m*/*z* 701 in the DP3 and DP4 fractions, respectively. As earlier with HPAEC-PAD analysis, some minor peaks were also observed in the MS spectra.

The DP3 fraction was further analyzed by ESI-MS/MS to get more structural information from the compounds in this fraction and on the oligomeric products in general. The base peak of the DP3 fraction (*m*/*z* 539) was confirmed to be a cellotriose (Glc3) by comparing the MS/MS spectrum with the cellotriose standard spectrum (Fig. 4A). Precursor ion of *m*/*z* 521 was identified as a dehydration product of cellotriose $[Glc3-18\ Da+Cl]^-$. In the MS/MS spectrum of this compound, cross-ring cleavage fragmentation products were not observed. Generally, the cross-ring fragments are formed from reducing oligosaccharides if a chloride adduct is attached and the absence of them indicates that the dehydrated compound does not have an anomeric carbonyl group available for retro-aldol reaction.[25] Thus the MS results suggest a 1,6-anhydrous structure without the anomeric carbonyl group, that is, cellobiose-levoglucosan, for the ion *m*/*z* 521 (Fig. 4B). The formation of the 1,6-anhydroglucose (levoglucosan) has been reported in the supercritical water treatment of cellulose,[26] and cellobiose[27,28] by hydrolysis and dehydration reactions, and was also detected in this study (see below). 1,6-anhydro-β-D-cellooligosaccharides (β-D-glucopyranosyl$_n$-levoglucosans) from cellulose were earlier found by Ehara and Saka.[17]

Two other minor compounds, *m*/*z* 479 and *m*/*z* 451 ions, were identified as cross-ring fragmented products from the reducing end of cellotriose. Based on their MS/MS spectra, the *m*/*z* 479 ion (Fig. 4C) was identified as cellobiose–erythrose by loss of 60 Da glycolaldehyde ($C_2H_4O_2$). The *m*/*z* 451 (Fig. 4D) ion was identified as hemiacetal form of cellobiose-glycolaldehyde and methanol present in the MS solvent $[Glc3-120\ Da+MeOH+Cl]^-$. Small amount of cellobiose–glycolaldehyde hydrate (hemiacetal with water) *m*/*z* 437/599 $[Glc3/4-120\ Da+H_2O+Cl]^-$ and cellobiose–glycolaldehyde *m*/*z* 419/581 $[Glc3/4-120\ Da+Cl]^-$ were also identified in the MS spectra (Fig. 3). Similar findings of hydrates of degradation products have recently been reported applying HPAEC-PAD–MS.[28]

The degradation products identified in the ESI-MS/MS analysis were linked to their corresponding peaks in Figure 2 by employing the HPAEC-PAD analysis coupled with mass spectrometry (HPAEC-PAD–MS). Thus the HPAEC-PAD–MS analysis revealed the following elution order of the cello-oligosaccharides and their degradation products: Glc$_n$ −18 Da, Glc$_n$ −120 Da, Glc$_n$, and Glc$_n$ −60 Da, where Glc$_n$ is the corresponding cello-oligosaccharide. In particular, the α- and β-peaks in Figure 2 were found to be glucosyl$_n$-levoglucosan (−18 Da) and glucosyl$_n$-erythrose (−60 Da), respectively. The lack of reducing end group in the dehydrated products

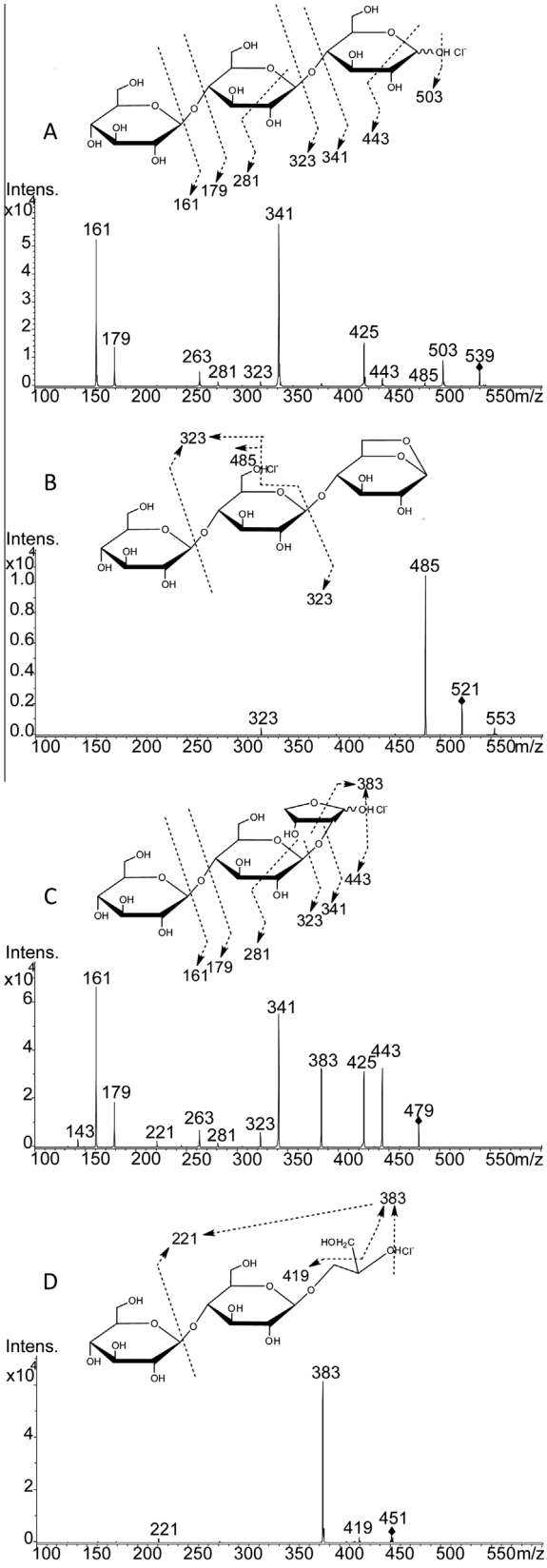

Figure 4. ESI-MS/MS spectra of fraction 53 (DP3) and proposed fragmentation pathways of (A) cellotriose (m/z 539), (B) 1,6-anhydro-β-D-cellotriose (cellobiose–levoglucosan) (m/z 521), (C) cellobiose–erythrose (m/z 479), and (D) cellobiose–glycolaldehyde (m/z 451) as chloride adduct ion. The actual position of chloride anion is unknown.

(glucosyl$_n$-levoglucosan) is indeed expected to result in limited retention in the HPAEC column. As Glc$_n$ and Glc$_n$ −120 Da elute very closely, their order may vary depending on the column (CarboPacPA100, CarboPacPA200) and applied elution conditions.

Low molar mass constituents from each of the non-fractionated samples were analyzed via the GC–MS, which resulted in the identification and quantification of several C4–C6 carbohydrates and their lower fragments, aliphatic hydroxy or oxocarboxylic acids, and miscellaneous compounds (Table 3). In addition, several other compounds could be only partially characterized or they remained totally unknown.

In the GC–MS chromatograms, up to ten peaks were found eluting between the glucopyranose and cellobiose peaks. Their mass spectra exhibited an intense m/z 361 peak, characteristic of trimethylsilylated hexose disaccharides and related compounds.[29,30] It is therefore reasonable to assume that they represent partially fragmented cellobiose, such as glucosyl-erythrose and glucosyl-glycolaldehyde, which supports our results from HPAEC-PAD–MS and ESI-MS/MS measurements and is in agreement with the literature.[27] Also the detected fructose, levoglucosan, erythrose, dihydroxyacetone, and glycolaldehyde are well-established products from the sub- and supercritical water treatment of cellulose,[17,31] cellobiose,[16] and glucose.[32]

The main identified monomeric carbohydrates included fructose, levoglucosan, mannose, xylose, and erythrose, but small amounts of xylulose were also present. The fragments of lower molar mass included glycolaldehyde, found in two dimeric forms,[20] and monomeric dihydroxyacetone. The presence of mannose and xylose, and its isomer xylulose, can readily be explained as trace impurities in the applied cellulose material, although some mannose may also be formed by isomerization of glucose-derived fructose.

Several carbohydrates or carbohydrate-derived compounds, usually found in small amounts, could be only partially characterized. Their mass spectra as the TMS derivatives usually contained several ions characteristic of carbohydrate derivatives (e.g., those at m/z 204, 205, 217 and 218), but in many cases intense atypical ion peaks were also found (e.g., m/z 155 or 348) hampering final identifications. It is possible that at least some of them represent mixed dimers of glycolaldehyde, methylglyoxal, dihydroxyacetone, or glyceraldehyde.[33]

Table 3
Minor degradation products formed from cello-oligosaccharides (mg mL^{-1})

Compound	0.2 s	0.4 s	0.6 s
Levoglucosan	3	8	5
Fructose	3	7	8
Xylose	2	3	4
Xylulose	<1	<1	<1
Erythrose	2	4	3
Dihydroxyacetone	<1	<1	<1
Glycolaldehyde	1	2	2
Other sugar-type compd	2	3	5
Glycolic acid	4	5	4
Lactic acid	<1	1	<1
Pyruvic acid	<1	<1	<1
Glyceric acid	<1	<1	<1
2,4-Dihydroxybutanoic	<1	<1	<1
Erythronic acid	<1	<1	<1
Gluconic acid	<1	<1	<1
5-Hydroxymethylfurfural	<1	2	1
Reductic acid (tentative)	<1	1	1
Catechol	<1	<1	<1
Pyrogallol	<1	<1	<1
Miscellaneous	2	3	3

Of the non-volatile aliphatic carboxylic acids, only glycolic acid occurred in moderate amounts (Table 3). It has frequently been found, together with lactic and pyruvic acids, after the sub- and supercritical water treatments of cellulose or cellulosic materials, for example, by Yoshida et al.[34] The identified glyceric, 2,4-dihydroxybutanoic, erythronic, and gluconic acids represent known oxidation or fragmentation products of different carbohydrates of which the 2,4-dihydroxybutanoic acid is typically formed during alkaline treatments.

3.4. Summarizing remarks

The current results show that crystalline cellulose is dissolved and depolymerized in supercritical water treatment forming dissolved polymers, which are insoluble in ambient water, ambient-water-soluble cello-oligosaccharides, monosaccharides, and degradation products thereof. In the present study, the maximum yield of undegraded cello-oligosaccharides was 42%, which compares well with the yields of 32% for oligosaccharides and 47% for total water-soluble sugars reported by Ehara and Saka with a single-stage treatment for 0.2 s at 400 °C.[31] Zhao et al. have also reported a 39% yield of DP2-5 oligosaccharides using a batch reactor at 380 °C for 16 s.[26]

In supercritical water the depolymerization of dissolved cellulose chains occurs according to a random cleavage of the glycosidic bonds owing to the detected Flory–Schulz type of distribution of the formed cello-oligosaccharides. Depolymerization via hydrolysis is not, however, the only degradation mechanism in supercritical water treatment. Also thermal chain cleavage without water addition results in the formation of a cello-oligosaccharide with a levoglucosan end group, and dehydration and fractionation reactions take place in the reducing end groups as in the present and earlier studies show.[35] In general, the quantity of degraded compounds increased when treatment time is extended. This is due to the dehydration and fractionation of the end groups but also due to the formation of new end groups by the hydrolytic depolymerization, which become susceptible to aforementioned reactions. On the contrary, when the treatment time is very short, the amount of degraded AGUs can be limited to less than 4%; at the same time a significant amount of the dissolved cellulose typically remains insoluble in ambient water.[12,36,37]

To obtain an optimal yield of water-soluble cello-oligosaccharides it is essential to optimize the treatment conditions in a way which minimizes the formation of the water-insoluble precipitate, the monomeric sugars and their degradation products. The fragmentation reactions become more favored over hydrolysis reactions in supercritical water compared with subcritical water.[15,31] Therefore it may be preferable to limit supercritical water treatment only for the dissolution of the cellulose crystallites, and carry out the final hydrolysis to water-soluble oligomers in subcritical water. This has been demonstrated by Ehara and Saka with promising results in terms of a low concentration of unwanted degradation products.[31] On the other hand, the formation of furfurals and phenols through dehydration is known to be pronounced under ionic conditions in subcritical water.[15] Therefore, a short treatment in near critical or supercritical water appears desirable in order to reduce the overall treatment time and avoid the formation of furfurals and phenols which are known to polymerize easily resulting in humin or soot formation.

4. Conclusions

Supercritical water treatment appears to be a promising process for the manufacture of water-soluble cello-oligosaccharides. The present study demonstrated this at the temperature of 380 °C and at the pressure of 250 bar using treatment times of 0.2–0.6 s, with the highest yield of 42% for DP2-9 cello-oligosaccharides after 0.4 s of treatment. The residual reaction products also consisted of 11% precipitate with a DP_w of 16, and 6.1% monomeric sugars. Attention was paid to the structural analysis of oligomeric and monomeric degradation products. It was shown that cello-oligosaccharides contain fragmented (glucosyl$_n$-erythrose, glucosyl$_n$-glycolaldehyde) and dehydrated (glucosyl$_n$-levoglucosan) sugar end-groups. These derivatives may limit the use of such oligosaccharide product, for example, in human foods.

Acknowledgments

The authors would like to acknowledge Sanna Koutaniemi for her help with the preparative size exclusion chromatography, Tarja Tamminen for discussions and interpretation of the data, and Seppo Jääskeläinen and his crew for their efforts with the reactor system. This work was funded by the Finnish Funding Agency for Technology and Innovations (TEKES), and Finnish Bioeconomy Cluster Ltd as a part of the Future Biorefinery Program.

Supplementary data

Supplementary data (molar mass distributions of cellulose precipitate, a description of the extended calibration method used for DP7-9 cello-oligosaccharides, and the HPAEC-PAD and HPAEC-PAD–MS chromatograms of the discussed analyses) associated with this article can be found, in the online version, at http://dx.doi.org/10.1016/j.carres.2014.10.012.

References

1. Klemm, D.; Heublein, B.; Fink, H.; Bohn, A. *Angew. Chem., Int. Ed.* **2005**, *44*, 3358–3393.
2. Roberfroid, M. *J. Nutr.* **2007**, *137*, 830S–837S.
3. Mussatto, S. I.; Mancilha, I. M. *Carbohydr. Polym.* **2007**, *68*, 587–597.
4. Cardenas-Toro, F. P.; Alcazar-Alay, S. C.; Forster-Carneiro, T.; Meireles, M. A. A. *Food Publ. Health* **2014**, *4*, 123–139.
5. Nakamura, S.; Oku, T.; Ichinose, M. *Nutrition* **2004**, *20*, 979–983.
6. Gross, A. S.; Chu, J. *J. Phys. Chem. B* **2010**, *114*, 13333–13341.
7. Bergenstråhle, M.; Wohlert, J.; Himmel, M. E.; Brady, J. W. *Carbohydr. Res.* **2010**, *345*, 2060–2066.
8. Adschiri, T.; Hirose, S.; Malaluan, R.; Arai, K. J. *Chem. Eng. Japan* **1993**, *26*, 676–680.
9. Yu, Y.; Wu, H. *Energy Fuels* **2010**, *24*, 1963–1971.
10. Tolonen, L. K.; Zuckerstatter, G.; Penttilä, P. A.; Milacher, W.; Habicht, W.; Serimaa, R.; Kruse, A.; Sixta, H. *Biomacromolecules* **2011**, *12*, 2544–2551.
11. Deguchi, S.; Tsujii, K.; Horikoshi, K. *Green Chem.* **2008**, *10*, 191–196.
12. Sasaki, M.; Adschiri, T.; Arai, K. *AIChE J.* **2004**, *50*, 192–202.
13. Tolonen, L. K.; Penttilä, P. A.; Kruse, A.; Serimaa, R.; Sixta, H. *Cellulose* **2013**, *20*, 2731–2744.
14. Cantero, D. A.; Bermejo, M. D.; Cocero, M. J. *J. Supercrit. Fluids* **2012**, *75*, 48–57.
15. Kruse, A.; Gawlik, A. *Ind. Eng. Chem. Res.* **2003**, *42*, 267–279.
16. Sasaki, M.; Furukawa, M.; Minami, K.; Adschiri, T.; Arai, K. *Ind. Eng. Chem. Res.* **2002**, *41*, 6642–6649.
17. Ehara, K.; Saka, S. *Cellulose* **2002**, *9*, 301–311.
18. Testova, L.; Chong, S.; Tenkanen, M.; Sixta, H. *Holzforschung* **2011**, *65*, 535–542.
19. Borrega, M.; Niemelä, K.; Sixta, H. *Holzforschung* **2013**, *67*, 863–870.
20. Novina, R. *Chromatogrophia* **1984**, *18*, 96–98.
21. Havlicek, J.; Peterson, G.; Samuelson, O. *Acta Chem. Scand.* **1972**, *26*, 2205–2215.
22. Yu, Y.; Wu, H. *Ind. Eng. Chem. Res* **2009**, *48*, 10682–10690.
23. Baumgarten, J. L.; Busnel, J. P.; Meira, G. R. *J. Liq. Chromatogr. Related Technol.* **2002**, *25*, 1967–2001.
24. Flory, P. J. *J. Am. Chem. Soc.* **1936**, *58*, 1877–1885.
25. Vinueza, N. R.; Gallardo, V. A.; Klimek, J. F.; Carpita, N. C.; Kenttämaa, H. I. *Fuel* **2012**, *105*, 235–246.
26. Zhao, Y.; Lu, W.; Wang, H. *Chem. Eng. J.* **2009**, *150*, 411–417.
27. Kabyemela, B. M.; Takigawa, M.; Adschiri, T.; Malaluan, R. M.; Arai, K. *Ind. Eng. Chem. Res.* **1998**, *37*, 357–361.
28. Yu, Y.; Shafie, Z. M.; Wu, H. *Ind. Eng. Chem. Res.* **2013**, *52*, 17006–17014.
29. Niemelä, K. *Carbohydr. Res.* **1989**, *194*, 37–47.
30. Kochetkov, N. K.; Chizhov, O. S.; Molodtsov, N. V. *Tetrahedron* **1968**, *24*, 5587–5593.
31. Ehara, K.; Saka, S. *J. Wood Sci.* **2005**, *51*, 148–153.
32. Kabyemela, B. M.; Adschiri, T.; Malaluan, R. M.; Arai, K. *Ind. Eng. Chem. Res.* **1999**, *38*, 2888–2895.

33. Gardiner, D. *Carbohydr. Res.* **1966**, *2*, 234–239.
34. Yoshida, K.; Miyafuji, H.; Saka, S. *J. Wood Sci.* **2009**, *55*, 203–208.
35. Matsumura, Y.; Sasaki, M.; Okuda, K.; Takami, S.; Ohara, S.; Umetsu, M.; Adschiri, T. *Combust. Sci. Technol.* **2006**, *178*, 509–536.
36. Sasaki, M.; Iwasaki, K.; Hamaya, T.; Adschiri, T.; Arai, K. *Kobunshi ronbunshu* **2001**, *58*, 527–532.
37. Cantero, D. A.; Bermejo, M. D.; Cocero, M. J. *Bioresour. Technol.* **2012**, *135*, 697–703.